OPEN ACCESS

International
Journal
Of Modern Engineering Research (IJMER)

Calculation of Neutron Density Distributions of Tin Isotopes Using the Thomas-Fermi Approximation

E. Eser[1], A. Yalcin[2], M.H. Bolukdemir[3], M. Gokbulut[2], H. Koc[4]

[1] *Department of Physics, Polatlı Faculty of Arts and Sciences, Gazi University, Turkey*
[2]*Department of Physics, Faculty of Arts and Sciences, Gaziosmanpaşa University, Turkey*
[3]*Department of Physics, Faculty of Sciences, Gazi University, Ankara, Turkey*
[4] *Department of Electrical and Electronics Engineering, Faculty of Engineering, Muş Alparslan University, Turkey*

ABSTRACT: *In this work, the neutron density distributions of some tin isotopes ($^{116, 118, 120, 124, 132}$Sn) have been calculated by using a simple analytical expression obtained for the Fermi integral which is situated in the nucleon density distributions. The obtained results are compared with the available theoretical and experimental data in the literature, and were found in agreement. The obtained results demonstrated the analytical expression can be used to the neutron density distributions.*
Keywords: *Neutron density distribution, Sn-isotopes, Thomas-Fermi approximation*

I. INTRODUCTION

Knowledge of protons and neutron densities in nuclei is crucial for our understanding of the fundamental properties of nuclei [1-4]. Also, the nucleon density is a directly related to the size of an atomic nucleus and plays an important role in the cross sections of nuclear reactions therefore, to achieve a form of nuclear densities on algebraic is of great importance particularly for the analytic studies of the nuclear scattering and reaction processes [5, 6].

The information about the proton densities in nuclei may be derived from studies of the nuclear charge, the nuclear scattering and reactions, isobaric energy shifts, electron scattering and the muon scattering [7]. Nuclear charge densities in general expressed by using Fourier Bessel series, harmonic oscillator distribution, two or three parameter Gaussian distribution and Fermi distribution [8, 9]. To describe nuclear charge densities the most used distributions are Fermi and Gaussian distributions and the Gaussian distribution is suitable for describing the charge densities of light nuclei while Fermi-type distribution is more suitable for heavier nuclei [10].

In contrast to the proton densities, the information about the neutron densities is rather scarce and is exactly not known even in the stable nuclei. Because neutrons are uncharged particles, the measurement of their spatial distribution in the nucleus is more difficult than for the positively charged protons so our knowledge about the neutron distribution and its rms radius in nuclei is not so precise [5, 11]. Experimental studies in order to obtain the neutron densities are usually involves strongly interacting hadronic probes, such as proton nucleus elastic scattering, α-particle or pion elastic scattering, and techniques based on the inelastic scattering excitation of the giant dipole and spin-dipole resonances [11]. For strongly interacting particles used in these studies, analysis of the scattering data varies depending on the model and the results are very sensitive to uncertainties in the approach to the many body scattering theories [12]. The most important reason that the nuclear environment, the lack of information about the nucleon-nucleon scattering amplitudes [13].Consequently the information about the neutron distributions is comparatively less reliable and is rather scarce [9].

Many experimental and theoretical studies have been done to gain empirical information about neutron and proton densities in nuclei [1,5,7,11,13-24]. Gills and Rebel [19] report on investigations of elastic scattering of 104 MeV alpha-particles from Pb-204-206-208 looking for information on the neutron distributions and on isotopic differences and the differential cross sections are carefully measured with high angular accuracy which is necessary for the intended analyses. Differential cross section of proton nucleus elastic scattering at intermediate energies have been measured in studies conducted by Zenihiro et al. [13], and information about both the nuclear surface and interior had been obtained. In studies using the interaction of antiprotons with nucleus, the neutron skin thickness of nuclei has also been investigated through radiochemical and x-ray techniques in antiprotonic atoms [11, 20-22].

Besides the experimental studies, a lot of theoretical studies have been made to explain the neutron distributions in nuclei. The density distribution of super-heavy nuclei with atomic number of 104 to 120 using the Skyrme-Hartree-Fock model was investigated by Pei et al. [5]and due to deformation it seen that proton densities and neutron density have central depressions. At theoretical studies made by Gambhir et al., [1,7] by considering the asymptotic behavior of the density, for neutron and proton densities were obtained from a simple semi-phenomenological expression.

Tin has many stable isotopes. The unstable tin isotopes have also a long isotopic chain including two double-magic nuclei. Moreover, its proton number is a magic number. Thus, because of the features of these privileged tin nuclei, tin isotopes are suitable for the study of systematic changes in neutron density distributions [25].

In the present study our aims show the ability of our method to predict the nucleon densities of nuclei as our study in Ref. [4]. For this reason, the neutron densities of even-even Sn isotopes (A=116-132) have been calculated using the Thomas-Fermi method with a new analytical expression obtained for the Fermi integral in Ref. [26].

II. THEORETICAL BACKGROUND

The nucleon distribution is given by [27, 28]:

$$\rho(r) = \frac{2}{h^3}\int n(\boldsymbol{r},\boldsymbol{p})d\boldsymbol{p} \tag{1}$$

$$= \frac{4\pi}{h^3}[2m^*(r)T]^{3/2}J_{1/2}\big(\eta(r)\big). \tag{2}$$

Where h is Planck constant, T is temperature, $J_F(\eta)$ is Fermi integrate and m^* is the effective nucleon mass [28],

$$m^* = m(m_k/m)(m_w/m). \tag{3}$$

$$J_F(\eta) = \int_0^\infty \frac{y^F}{1+\exp(y-\eta)}dy, \tag{4}$$

and

$$\eta(r) = \mu - V(r)/T\ . \tag{5}$$

In Eqs. (3) and (4), μ is the chemical potential and $V(r)$ is the effective single particle potential, which is given by

$$V(r) = V_{ws}(r) + V_l(r) + V_{ls}(r) + V_c(r). \tag{6}$$

In Eq. (6), the Woods-Saxon potential:

$$V_{ws}(r) = -V\left[1 + exp\left(\frac{r-R}{a}\right)\right]^{-1}. \tag{7}$$

Where N is the total number of neutrons in the nucleus, the surface thicknesses a is 0.7 fm, the mean radius of nuclei R is $R_0A^{1/3}$(R_0=1.347 for the neutrons) and [38]

$$V = V_0\left\{1 \pm K\left(\frac{N-Z}{A}\right)\right\}. \tag{8}$$

Here V_0 is the depth of potential well, K is 0.6553, Z and A are the proton number and the mass number, respectively. $V_I(r)$ is the isovector part of Woods–Saxon potential, which is defined as [38]

$$V_I(r) = 2\sigma V_{ws}(r)\left(\frac{N-Z}{A}\right)t_Z \tag{9}$$

In Eq. (9), the isovector parameter $\sigma = 0.63$ and t_Z is $\frac{1}{2}$ for the neutrons. The spin-obit potential [29]

$$V_{ls}(r) = \left(-\frac{\lambda V}{1+e^{(r-R)/a}}\right) \tag{10}$$

By taking the derivative of the first order of the spin-orbit potential in Eq. (10), its contribution to the system is added

$$\zeta\frac{1}{r}\frac{dV_{ls}(r)}{dr} = \zeta\frac{1}{r}\frac{d}{dr}\left(-\frac{\lambda V}{1+e^{(r-R)/a}}\right) \tag{11}$$

Here, the spin-orbital pair force $\zeta = 0.263\left(1 + 2\frac{N-Z}{A}\right)$, and λ is 36 for neutron. The Coulomb potential in Eq. (6) is given by:

$$V_c(r) = e^2(Z-1)\begin{cases} \frac{1}{2R}\left[3 - \left(\frac{r}{R}\right)^2\right], & r \le R \\ \frac{1}{r}, & r > R \end{cases}. \qquad (12)$$

where e^2=1.4399 (MeV.fm). For the calculation of the Fermi integral in Eq. (4), the series relation suggested in the previous paper [26] is as follows:

$$J_\alpha(\eta) = \frac{\eta^{\alpha+1}}{\alpha+1} + \lim_{N\to\infty}\sum_{i=0}^{N} f_i(-1)K_i(\alpha,\eta)$$

$$+ \lim_{N\to\infty}\sum_{j=0}^{N'} f_j(-1)e^{\eta(1+j)}\frac{\Gamma(\alpha+1,\eta(j+1))}{(j+1)^{\alpha+1}}, \quad 0 < \eta < \infty \qquad (13)$$

and

$$K_i(\alpha,\eta) = \begin{cases} \sum_{j=0}^{\alpha}(-1)^j f_j(\alpha)\eta^{\alpha-j}\frac{\gamma(j+1,i\eta)}{i^{j+1}}, & \text{integer } \alpha > 0 \\ \lim_{M\to\infty}\sum_{j=0}^{M}(-1)^j f_j(\alpha)\eta^{\alpha-j}\frac{\gamma(j+1,i\eta)}{i^{j+1}}, & \text{non integer } \alpha \end{cases}. \qquad (14)$$

In Eqs. (13) and (14), $\Gamma(\alpha,x)$ and $\gamma(\alpha,x)$ are gamma function and imcomplete gamma function, respectively [30]. Substituting Eq. (14) into Eq. (2), the formula for neutron density distributions can be obtained as follows:

$$\rho(r) = \frac{4\pi}{h^3}[2m^*(r)T]^{\frac{3}{2}} \times \frac{\eta^{\alpha+1}}{\alpha+1} + \lim_{N\to\infty}\sum_{i=0}^{N} f_i(-1)K_i(\alpha,\eta)$$

$$+ \lim_{N\to\infty}\sum_{j=0}^{N'} f_j(-1)e^{\eta(1+j)}\frac{\Gamma(\alpha+1,\eta(j+1))}{(j+1)^{\alpha+1}}. \qquad (15)$$

Taking into consideration the analytical expression (Eq.14) obtained for the Fermi integral; the neutron density distributions of Sn isotopes have been investigated.

III. RESULTS AND DISCUSSIONS

In the present study, it is calculated the neutron density distributions of Sn isotopes using a new analytical expression obtained for the Fermi integral in Ref [26]. This expression differs than other expressions and is simpler. The calculated neutron density distributions for Sn isotopes are shown in Figs. 1-5.Then, by comparing the obtained results with the experimental and with other theoretical results [14, 25, 31-35], we evaluated the consistency of our calculations. The agreement between the results provides a well starting point for making predictions of neutron and proton densities for other nuclei.

The adequacy of the graphics proves that the results are satisfactory. In our calculations we only used the value of the Fermi energy(obtained from the literature) at *T*=0 K for the chemical potential because of the Fermi energy at zero temperature is equals to the chemical potential. The Fermi energies for tin isotopes are calculated by using the Equation is given Ref. [4, 36, 37]:-8.187423 MeV for 116Sn, -7.67207 MeV for 118Sn, -7.622078 MeV for 120Sn, -6.946407 MeV for 124Sn and -7.31768 MeV for 132Sn.

Notice that, as we add more neutrons (going from 116Sn to 132Sn), the shape of the neutron-density distribution changes, also the depression at the center changes to a hump in the neutron distribution because of shell filling.

Fig. 1a shows the neutron density of $^{116}_{50}$Sn for different radius values. As shown in Fig. 1a, our calculations for $^{116}_{50}$Sn are consistent with the results of calculations from Ref. [32].For example our and Bartel et al. [32] results in r = 3.5 fm are0.08705 fm^{-3} and 0.08690 fm^{-3}, respectively. The great discrepancy between the results of our and Bartel et al. [30]is about 9% in r = 0.5 fm.The results obtained in this study also is consistent with Vautherin and Negele [33]'s theoretical results and Batty et al. [31]'s the experimental results. This agreement is increased in the radius range 1.5 fm– 6.0 fm. For example, the results of calculated and obtained from the literature in r = 3.5 fm are 0.04378 fm^{-3}, 0.04208 fm^{-3} [33], 0.03892 fm^{-3} [25], 0.04278 fm^{-3} [32], 0.04111 fm^{-3} [31], respectively. The discrepancy observed here could be from different assumptions used in each study models (potential selection and etc) or these deviations can be originates from the model of calculation.

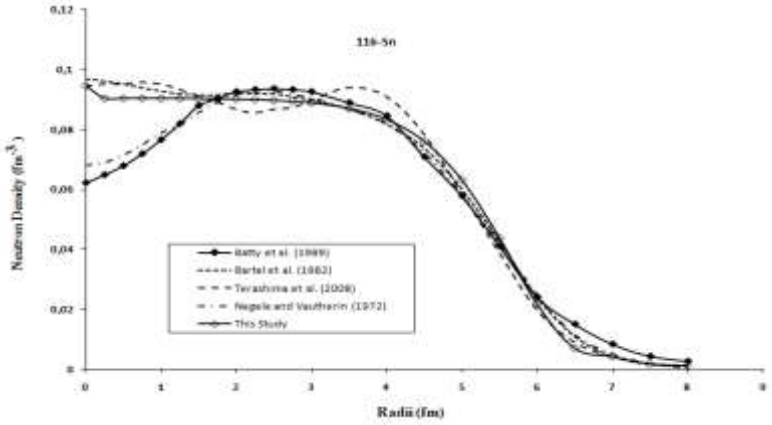

Fig. 1a. Neutron density distribution of ^{116}Sn

The neutron densities for different radius of $^{118}_{50}$Sn are shown in Fig. 1b. It is clearly seen that the calculated result is in harmony with the obtained results by Denisov and Nesterov [35]. For example, the results calculated and obtained from the literature in r = 4.5 fm are 0.07665 fm^{-3}, 0.07861 fm^{-3} [25] and 0.07783 fm^{-3} [35], respectively. The largest discrepancy observed between the calculated in this study and the results which obtained from Terashima et al. [25] obtained of is in r = 0.25 fm and equals to 4.89 %.

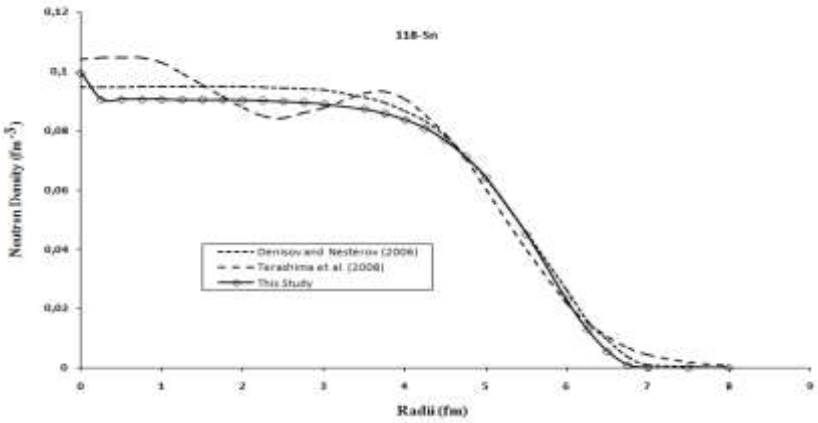

Fig. 1b. Neutron density distribution of ^{118}Sn

We show in Fig 1c the neutron density of $^{120}_{50}$ Sn depending the radii. It seen that the results obtained from this study is similar to those of Terashima et al. [25]. In r = 4.75 fm, the calculated and the literature results of $^{120}_{50}$ Sn are 0.07011 fm^{-3}, 0.06988 fm^{-3} [14] and 0.06982 fm^{-3} [25], respectively. It seen that the largest discrepancy between the calculated and other results is in r = 0.25 fm and equals to 19.39%.

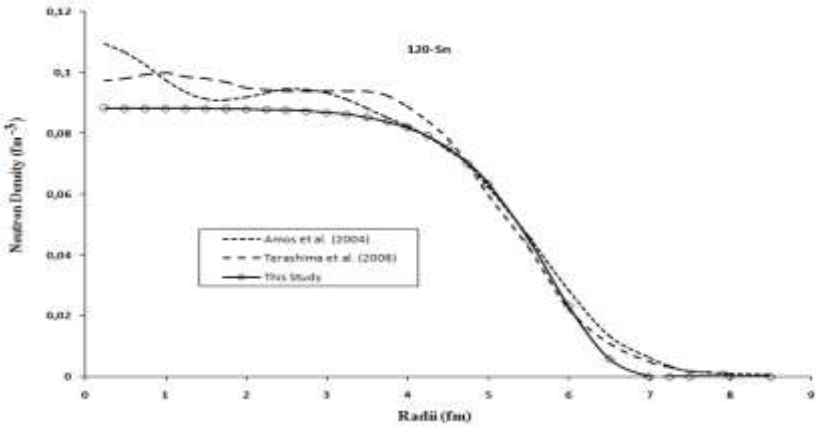

Fig. 1c. Neutron density distribution of ^{120}Sn

Fig. 1d show the calculated and literature results obtained for the neutron density distribution of $^{124}_{50}$ Sn [25, 33, 35]. As shown in the Fig. 1d, the results obtained in this study are in agreement with the results of Denisov and Nesterov [35]. In both studies, the distribution of the density is constant up to r = 4 fm and then decreases. Compared with other studies, the largest inconsistency between the values obtained is at r =0.25 fm and equals to 23.37%.

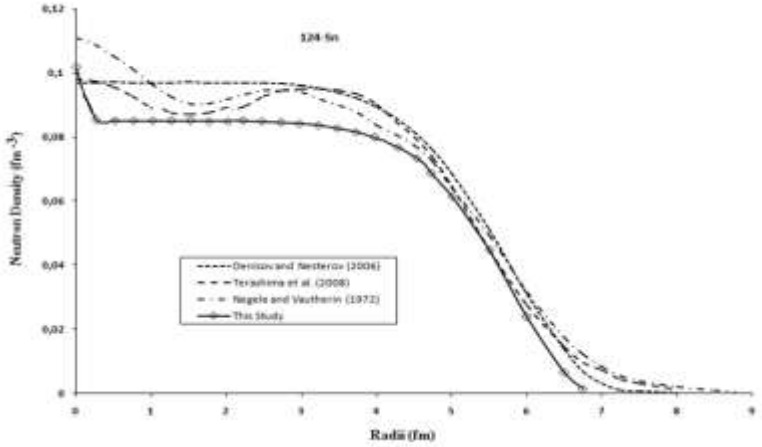

Fig. 1d. Neutron density distribution of ^{124}Sn

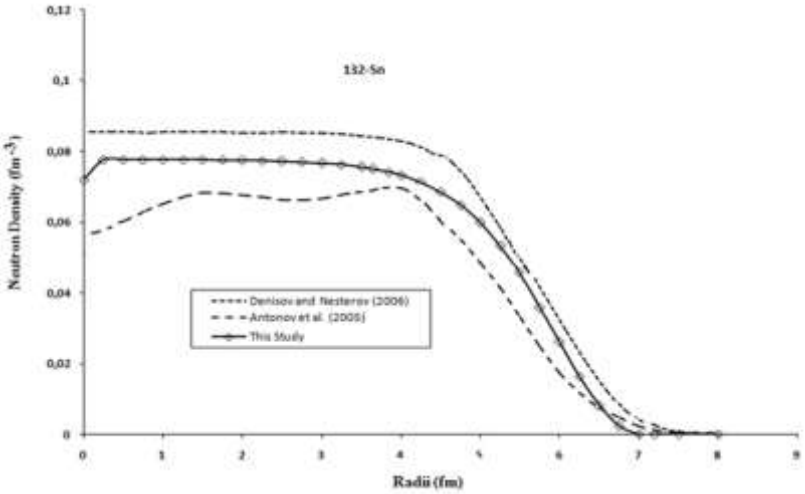

Fig. 1e. Neutron density distribution of ^{132}Sn

The calculated and literature results for the neutron density distribution of $^{132}_{50}$ Sn are shown in Fig. 1e. Our calculations are in agreement with those of Denisov and Nesterov [35] and this agreement is increased after r = 4.5 fm. The largest uncertainty is at r = 0.25 fm and equals to 27%.

Notice that, as we add more neutrons (going from ^{116}Sn to ^{132}Sn), we see uncertainty in the evolution of these densities contrast to the results given in Ref. [39]. In study of their, the densities of this nuclei increase with the number of neutrons. This uncertainty is caused by the different potentials used in models, and some interactions such as spin-orbit and symmetry effects take no account.

Even though there are some uncertainties between the results, the results obtained here show the ability of our method to predict the nucleon densities of nuclei. When more appropriate potential and parameters for the Sn isotopes are selected, more definite conclusions will be obtained.

The results obtained in the surface part of radii to compare to the middle value of the radius also are not satisfactory. Because the Thomas-Fermi method is not applicable to regions where the nuclear density changes, and the TF model is correct only in the limit of an infinite nuclear charge.

IV. CONCLUSION

We have investigated the neutron density distributions of some Sn isotopes (116, 118, 120, 124, 132) using a simple analytical expression [4, 26]. This study has shown that the analytical expression used gives a very reasonable description of the neutron densities of the Sn isotopes. Also, the results show that the presented methods for calculation of nucleon densities are computationally efficient and can avoid computational and time overflow. Therefore, the method used in the study can be used in future calculations for nucleon densities of other nuclei. In particularly, this approximation may provide a simple and efficient way to calculate nucleon densities.

ACKNOWLEDGEMENTS

We are very thankful to Prof. Dr. Cevad Selam for supplying some of the values used in our calculations and valuable comments in the work.

REFERENCES

[1]. Gambhir YK, Patil SH. Some characteristics of nuclear densities. Z. Phys. A-Atomic Nuclei 1986, 324: 9-13.

[2]. Dobaczewski J, Nazarewicz W, Werner T R, Berger J F, Chinn CR, Dechargé J. Mean-field description of ground-state properties of drip-line nuclei: Pairing and continuum effects. Physical Review C 1996,53: 2809-2840.

[3]. Yoshida S and Sagawa H. Neutron skin thickness and equation of state in asymmetric nuclear matter, Physical Review C 2004, 69: 024318.

[4]. Gokbulut M, Koc H, Eser E, Yigitoglu I and Mamedov B A. Investigations of density distributions of 208Pb with the Thomas-Fermi method. Modern Physics Letters A 2013, 28: 1350108.

[5]. Pei J C, Xu F R and Stevenson P D. Density distributions of superheavy nuclei. Physical Review C 2005, 71: 034302.

[6]. Gambhir Y K, Ring P, De Vries H. Semi-Phenomenological Charge Distributions in Nuclei. Europhysics Letters1989, 10: 219-224.

[7]. Gambhir Y K, Patil S H. Neutron and proton densities in nuclei. Z. Phys. A-Atomic Nuclei 1985, 321: 161-164.

[8]. Wong SSM. Introductory Nuclear Physics. WILEY-VCH Verlag GmbH&Co, Germany. 469 p, (2004).

[9]. Lalazissis G A, Panos C P, Grypeos M E, Gambhir Y K. Semi-phenomenological neutron density distributions. Z.Phys. A-Atomic Nuclei 1997, 357: 429-432.

[10]. Chu Y, Ren Z, Wang Z, Dong T. Central depression of nuclear charge density distribution. Physical Review C 2010, 82: 024320.

[11]. Warda M, Vinas X, Roca-Maza X, Centelles M. Analysis of bulk and surface contributions in the neutron skin of nuclei. Physical Review C 2010, 81: 054309.

[12]. RayL and Hodgson P E. Neutron densities and the single particle structure of several even-even nuclei from Ca^{40} to Pb^{208}. Physical Review C 1979, 20: 2403-2417.

[13]. Zenihiro J, Sakaguchi H, Murakami, Yosoi M, Yasuda Y, Terashima S, Iwao Y, Takeda H, Itoh M, Yoshida H P and Uchida M. Neutron density distributions of $Pb^{204,206,208}$ deduced via proton elastic scattering at Ep=295 MeV. Physical Review C 2010, 82: 044611.

[14]. Amos K, Karataglidis S, Dobaczewski J. Probing the densities of Sn isotopes. Physical Review C 2005, 70: 024607.

[15]. Krasznahorkay A, Akimune H, van den Berg A M, Blasi N, Brandenburg S, Csatlo´s M, Fujiwara M, Gulya´s J, Harakeh M N, Hunyadi M, de Huu M, Ma´te Z, Sohler D, van der Werf S Y, Wo¨rtche H J, Zolnai L. Neutron-skin thickness in neutron-rich isotopes. Nuclear Physics A 2004, 731: 224-234.

[16]. Hoffmann G W, Ray L, Barlett M, McGill J, Adams G S, Igo G J, Irom F, Wang A T M, Whitten C A, Boudrie R L, Amann J F, Glashausser C, Hintz N M, Kyle G S and Blanpied G S. 0.8 GeV p+Pb208 elastic scattering and the quantity Δ rnp. Physical Review C 1980, 21: 1488-1494.

[17]. Starodubsky V E and Hintz N M. Extraction of neutron densities from elastic proton scattering by Pb 206, 207, 208 at 650 MeV. Physical Review C 1994, 49: 2118-2135.

[18]. Donnelly T W and Walecka J D. Electron Scattering and Nuclear Structure. Annu. Rev. Nucl. Part. Sci. 1975, 25: 329-405.

[19]. Gils H J and Rebel H. Differences between neutron and proton density rms radii of Pb204, 206, 208 determined by 104 MeV α particle scattering. Physical Review C 1975, 13: 2159-2165.

[20]. Schmidt R, Czosnyka T, Gulda K, Hartmann F J, Jastrzebski J, Ketzer B, Klos B, Kulpa J, Kurcewicz W, Lubinski P, Napiorkowski P, Pienkowski L, Smolanczuk R, Trzcinska A, Von Egidy T, Widmann E and Wycech S. Determination of the proton and neutron densities at the nuclear periphery with antiprotonic X-rays and *p* -nucleus reactions. Hyperfine Interactions 1999, 118: 67-72.

[21]. Trzcinska A, Jastrzebski J, Lubinski P, Hartmann F J, Schmidt R, VonEgidy T, Klos B. Neutron Density Distributions Deduced from Antiprotonic Atoms. Physical Review Letters 2001, 87: 082501.

[22]. Kłos B, Trzcińska A, Jastrzębski J, Czosnyka T, Kisieliński M, Lubiński P, Napiorkowski P, Pieńkowski L, Hartmann F J, Ketzer B, Ring P, Schmidt R, von Egidy T, Smolańczuk R, Wycech S, Gulda K, Kurcewicz W, Widmann E, and Brown B A. Neutron density distributions from antiprotonic Pb^{208} and Bi^{209} atoms. Physical Review C 2007, 76: 014311.

[23]. Ni D, Ren Z, Dong T, Qian Y. Nuclear charge radii of heavy and superheavy nuclei from the experimental α-decay energies and half-lives. Physical Review C 2013, 87: 024310.
[24]. Ni D, Ren Z. Effects of differences between neutron and proton density distributions on α-decay half-lives. Physical Review C 2015, 92: 054322.
[25]. Terashima S, Sakaguchi H, Takeda H, Ishikawa T, Itoh M, Kawabata T, Murakami T, Uchida M, Yasuda Y, Yosoi M, Zenihiro J, Yoshida H P, Noro T, Ishida T, Asaji S and Yonemura T. Physical Review C 2008, **77**: 024317.
[26]. Guseinov I I and Mamedov B A. Unified treatment for accurate and fast evaluation of the Fermi–Dirac functions. Chin. Phys. B 2010, 19: 050501.
[27]. Samaddar S K, De J N, Vinas X, Centelles M. Density dependence of the symmetry free energy of hot nuclei. Physical Review C 2008, 78: 034607.
[28]. De J N, Shlomo S, Samaddar S K. Level density parameter in a refined Thomas-Fermi theory. Physical Review C 1998, 57: 1398.
[29]. Baran A. Relativistic mean field calculations of single particle potentials. Physical Review C 2000, 61: 024316.
[30]. Gradshteyn I S, Ryzhik I M. Tables of Integrals, Sums, Series and Product, Academic, New York, Vols. 340-345, pp. 662(1980).
[31]. Batty C J et al. In Advances in Nuclear Physics. Plenum, New York. Edited by J. W. Negele and E. Vogt. Vol. 19, p. 1. (1989).